Mathematical and Numerical Analysis of Droplet Surface Temperatures Using the Droplet Size Moment Theory

Sergio M. Hernandez-Gonzalez[1], A. Paul Watkins[2]
Department of Mechanical, Aerospace and Manufacturing Engineering, UMIST, Manchester, M60 1QD, United Kingdom.
[2]Tel: [44] (0) 161 200 3706.
[1]S.Hernandez-Gonzalez@postgrad.umist.ac.uk, [2]Paul.Watkins@umist.ac.uk

Determination of the surface temperature of droplets is key to obtaining the most accurate value of the heat transfer in a spray. Therefore, two different models to find the surface-averaged temperature of the droplets in a solid cone spray are introduced in this work. Such models are based on the theory of the moments of the droplet size distribution function introduced by Beck and Watkins. The transport equations for both liquid and gaseous phases are presented in a two-dimensional Eulerian form, and coupled through source terms, using the finite-volume approach. The behavior of the surface-averaged temperature agrees with that obtained by Abramzon and Sirignano. The fuel vapor mass fraction and the Sauter Mean Radius are also reported for the diverse cases studied in this work.

1. Introduction

The present study is based on the work done by Beck and Watkins [1] in which the moments of the droplet size distribution function are employed. The transport equations are written for the two moments that represent the liquid volume and surface area, which are the third and the fourth moments. The other two moments, representing total radius and droplet number, are approximated from a presumed distribution function, which is allowed to vary in space and time.

The present work concentrates only on the evaporation model of Beck and Watkins [2]. Such a model calculates the surface temperature by the 'third-rule' principle, which is based on the mean drop temperature and the mass fractions of fuel vapor and air. Also, the droplet surface properties are obtained based on this theory, neglecting then the direct influence of the surface temperature in the heat transfer process. Although accurate results have been achieved with this method for the convective heat transfer between the surface of the droplets and the surrounding gas, there is still uncertainty about the influence of the 'real' value of the surface temperature in such an energy transfer. This has led the present study to propose two different ways to model it. Both models are based on the droplet size moment theory.

2. General Overview of the Models and Assumptions

The two models proposed in this study use air as the carrier gas and assume an ideal spherical and homogeneous shape of the droplets. The first model also uses the Nusselt number proposed by Ranz and Marshall [3], which is based on the Reynolds and Prandtl numbers, whereas the second model uses that proposed by Chin and Lefebvre [4], involving the Spalding mass transfer number. Four fuels are tested for the first model and only n-dodecane is used for the second model. A range for fuel injection and gas temperature is considered, $293K \le T_{inj} \le T_{sat}$, where the saturation temperature depends on the fuel used in the analysis. The analyses are carried out under the assumption of a Lewis number of unity.

2.1 First Model

Assuming a spherical shape of droplets and considering them as 'solid spheres', a parabolic profile of temperature is employed so that variation of the temperature through the droplet is allowed and the surface temperature can then be found. The profile is given as follows

$$T = a + br + cr^2 \tag{1}$$

The constants a and b are found by evaluating the profile at the boundary conditions, such that $T = T_s$ at $r = r_s$ and $dT/dr = 0$ at $r = 0$. Whereas, the constant c is found by the definition of the liquid average temperature

$$\frac{\int_0^{r_s} Tr^2 dr}{\int_0^{r_s} r^2 dr} = T_l \tag{2}$$

Therefore, the final form of the parabolic profile is

$$T = T_s - \frac{5}{2}(T_s - T_l)\left[1 - \left(\frac{r}{r_s}\right)^2\right] \tag{3}$$

The heat transferred by conduction into the droplets is evaluated at the droplet surface ($r = r_s$) and the temperature profile can be used to find the gradient of temperature. This heat is then integrated over all droplets using the droplet moment theory, giving

$$Q_{in} = 20\pi k_l (T_s - T_l) Q_1 \tag{4}$$

Where Q_1 is locally the sum of the drop radii. Thus, the surface temperature is expressed as

$$T_s = T_l + \frac{Q_{in}}{20\pi k_l Q_1} \tag{5}$$

Heat transfer by convection is also involved since a gas surrounds the droplets. Firstly, the Nusselt number is defined [3] as

$$Nu = \frac{hD}{k_g} = 2 + 0.6\, Re^{1/2}\, Pr^{1/3} \tag{6}$$

Therefore, the convective heat transfer is

$$Q_{conv} = 2\pi r_s k_g (T_g - T_s)\left(2 + 0.6\, Re^{1/2}\, Pr^{1/3}\right) \tag{7}$$

The evaporative heat from the droplet is given by

$$Q_{ev} = \dot{m} L \tag{8}$$

Where the fuel vapor mass is given by $\dot{m} = 4\pi r_s D_c \rho_g \, ln(1 + B_M)$. As a unitary Lewis number is assumed, the evaporative heat becomes

$$Q_{ev} = 4\pi r_s \left(\frac{k}{c_p} \right)_g \ln(1 + B_M) L \tag{9}$$

It can be assumed that the heat used for heating up the droplets is given by the difference between the heat entering the droplet (convection) and the vaporizing heat. Then, this difference is integrated over all droplets following the moment droplet theory, resulting in

$$S_E = -2\pi k_g \left[(T_g - T_s) Nu_Q - 2\ln(1 + B_M) \frac{L}{c_{p\,g}} \right] Q_1 \tag{10}$$

Where

$$Nu_Q = 2 + 0.6\, Re_Q^{1/2}\, Pr^{1/3} \;\; ; \;\; Re_Q = \frac{2\rho_g V_{rel}}{\mu_g} \frac{Q_2}{Q_1} \tag{11}$$

Where Q_2 is the surface-area moment. By making an energy balance, Equation (10) is seen to be equal to the heat entering the droplet by conduction. Then, this equation is introduced into Equation (5) giving the surface temperature as

$$T_s = \frac{T_l + \alpha T_g}{1 + \alpha} \quad ; \quad \alpha = \frac{1}{10} \frac{k_g}{k_l} Nu_Q \tag{12}$$

This dimensionless parameter involves the thermal conductivities of both phases and the Nusselt number based on the moment droplet theory.

2.2 Second Model

The second model proposes a new transport equation for the surface temperature in the same pattern as the surface-area momentum equation introduced by Beck and Watkins [1]. The initial equation is given as

$$\rho_l \frac{D}{Dt}(T_k) = \frac{\partial}{\partial x_j} \left(\rho_l \sigma_v \nu_l \frac{\partial T_k}{\partial x_j} \right) - S_{Ek} \tag{13}$$

This equation is then treated algebraically and integrated over all droplets, becoming

$$\begin{aligned} &\frac{\partial}{\partial t} \int_0^\infty T_k r^k n(r) dr + \frac{\partial}{\partial x_j} \int_0^\infty T_k U_j r^k n(r) dr \\ &- \int_0^\infty T_k \left(\frac{\partial}{\partial t} \left(r^k n(r) \right) + \frac{\partial}{\partial x_j} \left(U_j r^k n(r) \right) \right) dr = \frac{\partial}{\partial x_j} \int_0^\infty \left(\sigma_v \nu_l r^k n(r) \frac{\partial T_k}{\partial x_j} \right) dr - S_{Ek} \end{aligned} \tag{14}$$

The moment droplet theory is applied to equation (14) obtaining the general form for the transport equations of temperature. The value of k giving the surface value is 2, resulting in

$$\frac{\partial}{\partial t}\left(Q_2 T_{l2}\right)+\frac{\partial}{\partial x_j}\left(T_{l2}U_{l2j}Q_2\right)+\frac{\partial}{\partial x_j}\left(\left(T_{l3}-T_{l2}\right)\left(U_{l3j}-U_{l2j}\right)Q_2\right)$$
$$+T_{l3}B_{Q_2}+T_{l2}\left(S_{Q_2}-B_{Q_2}\right)=\frac{\partial}{\partial x_j}\left(Q_2\sigma_v\nu_l\frac{\partial T_{l2}}{\partial x_j}\right)-S_{E2} \qquad (15)$$

Where T_{l2}, T_{l3}, U_{l3} and U_{l2}, represent the surface-averaged temperature, the volume-averaged temperature, the volume-averaged velocity and the surface-averaged velocity of the droplets, respectively. σ_v is the coefficient of Melville & Bray [5] and has a value of 0.7. The B_{Q2}, S_{Q2} and S_{E2} are the source terms due to break up (stripping and bag), changes in the surface area [6] and the energy, respectively. S_{E2} is given by

$$S_{E2}=\int_0^\infty\left[\frac{Q_{conv}-Q_{ev}}{\rho_l\cdot c_{p_l}\cdot r^3}\right]r^2 n(r)dr=\frac{4\pi k_g\ln\left(1+B_M\right)}{\rho_l\cdot c_{p_l}}\left[\frac{T_\infty-T_s}{B_M}-\frac{L}{c_{p_g}}\right]Q_0 \qquad (16)$$

where Q_0 represents the number of droplets, and the Nusselt number model is taken from [4].

3. Governing Equations

The transport equations for both liquid and gaseous phases are presented in a two-dimensional Eulerian form, and coupled through source terms, using the finite-volume approach [1]. The hybrid scheme is used to discretize these equations. A formulation for the fuel vapor mass fraction is also found in [2]. The $k-\varepsilon$ turbulence model is used for the gaseous phase in the model. The present research incorporates, in addition, either Equation (12) or (15). The injection conditions of the spray are given in Table 1.

Table 1. Injection Characteristics and Geometrical Parameter of the Nozzle and the Cylindrical Chamber

Quantity, Units	Value
Injection Pressure, MPa	17
Ambient Pressure, MPa	2
Nozzle Radius, mm	0.15
Axial Length of the Chamber, mm	100
Chamber Radius, mm	80
Injection Cell Length, mm	1
Inlet Droplet SMR, μm	7

4. Numerical Issues

The test cases involve a variety of temperatures for the carrier gas and the injected fuel. The iterative method used in this analysis to calculate the surface temperature by the first model with time step is based on the assumption that the surface temperature, T_s, at the beginning of the process is equal to the liquid average temperature. Then the value obtained is such that consecutive iterations satisfy the condition $\left|T_s^{j+1}-T_s^j\right|<0.3\,K$. The simulations are run using a time step of 2μs within a total time of the simulation of 5ms. The total CPU time required for every case is about 10 minutes on a PCG-GR55 due to the iterative internal process. The second model uses the Eulerian equations to calculate the surface temperature and, therefore, no internal iterative process is needed. This results in a less time-consuming process (around 6 minutes for each case using the same time step).

5. Results

The results presented are: a) the variations of the surface and liquid temperatures with time at a given axial distance from the nozzle, b) the droplet SMR obtained by considering all droplets at a given axial distance and, c) the centerline fuel vapor mass fraction.

5.1 First Model

Temperature

Figure 1 shows the variation of the surface-averaged and mass-averaged temperatures with time for n-dodecane at a point on the centerline 50mm from the injector. For n-octane and n-heptane, it is found that these parameter behave entirely similarly. Initial effects take place when liquid arrives to the cell, which contained only gas before. These effects are explained by the changes in pressure and specific volume of the gas, which is considered ideal. Also, the largest amount of liquid per time entering the cell is located at this time that the local pressure is being stabilized. Consequently, the void fraction decreases rapidly. These effects disappear after several time steps and, thereafter, a very well shaped curve of the variations of temperatures can be seen. The behavior of the liquid and surface temperatures agrees with that reported by Abramzon and Sirignano [7] and Daïf *et al.* [8].

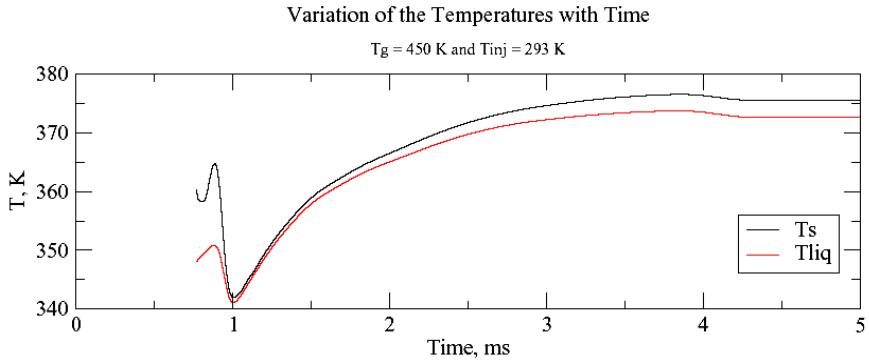

Figure 1. Variation of the Surface-Averaged and Mass-Averaged Temperatures with Time. (Model 1)

Figure 1 also shows that the surface-averaged and mass-averaged temperatures have a higher value than the injection temperature since the droplets are heated as they travel from the injector through the hot gas (450K or T_{sat}). In the case of high injection temperature and low ambient temperature, the surface- and mass-averaged temperatures have a lower value than the injection temperature since energy has been transferred to the carrier gas.

Sauter Mean Radius (SMR) and Fuel Vapor Mass Fraction (FVMF)

At low injection temperature (293K), the SMR increases as the gas temperature is increased (293K to T_{sat}) due to smaller droplets evaporating faster than the large droplets so that the SMR increases due to the complete evaporation of small droplets and only large droplets remain, see Figure 2a. The FVMF, Figure 3a, increases as the temperature is increased. This increase occurs because the gas exchanges more energy with the liquid heating the droplets faster so that they evaporate more quickly. The exponential increase in the FVMF reflects the increase in the rate of mass exchange as the droplet temperature increases.

As the injection temperature approaches the saturation temperature, the droplets size is found to be much smaller due to the large droplets experiencing appreciable evaporation and the sizes are much the same in each case, see Figure 2b. The FVMF along the axial distance in

the centerline, Figure 3b, can be seen to be much greater in these cases due to the liquid evaporating at a fast rate immediately after injection. For all the fuels, the spray is found to be more radially spread at large axial distance, which is reflected in the reduction of the FVMF along the axis. This decrease is also justified by the reduction of the rate of evaporation due to the cooling of the surrounding gas as it loses heat to the droplets in order that they may evaporate.

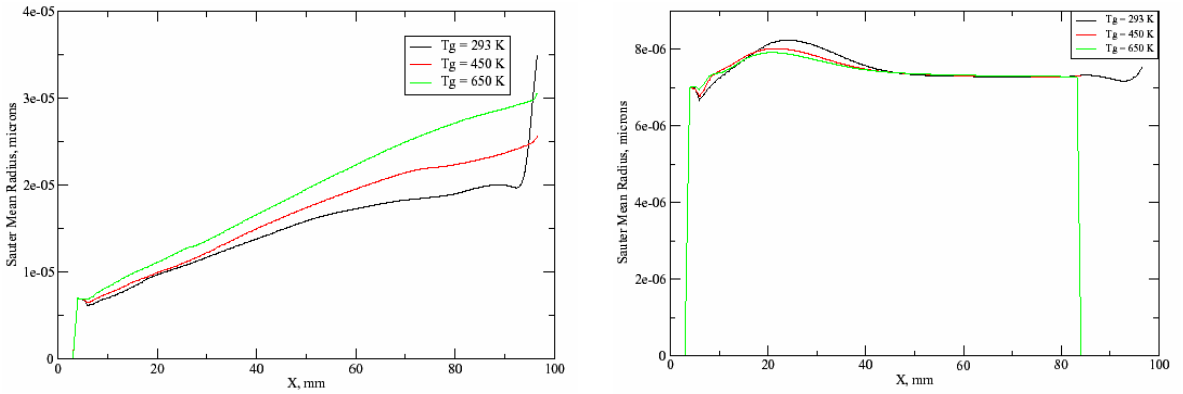

Figure 2. Variation of the SMR along the Axial Distance for n-Dodecane a) T_{inj} = 293K and b) T_{inj} = 650K.

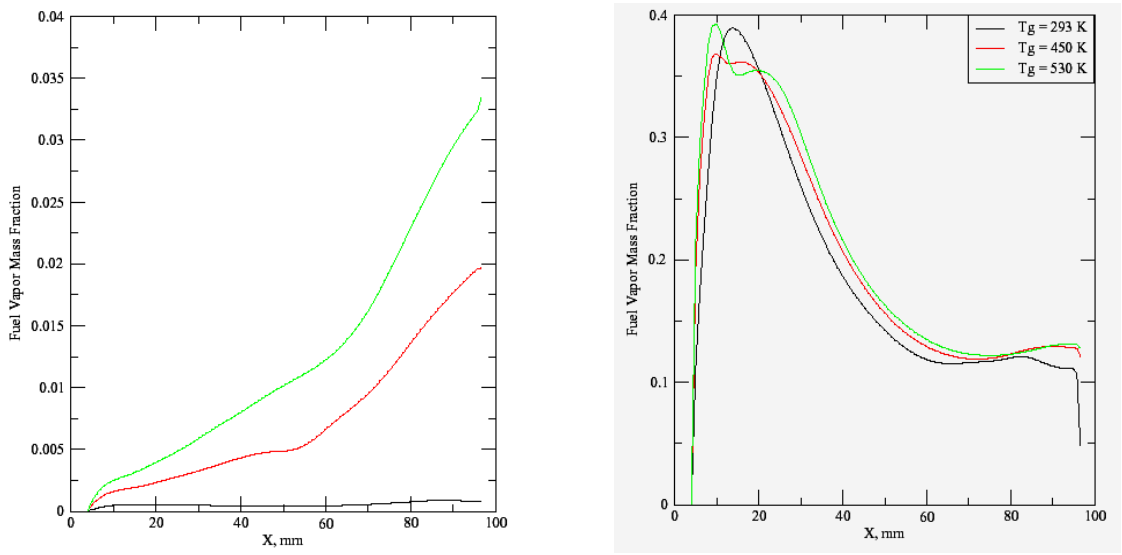

Figure 3. Variation of the FVMF along the Axial Distance for n-Octane a) T_{inj} = 293K and b) T_{inj} = 530K.

5.2 Second Model

Temperature

Figure 4 shows the variation of the liquid, gas and surface temperature with time for n-dodecane at a point on the centerline 50mm from the injector. Initial effects take place in this model too and can be explained by the same reasons as for the first model. The liquid and the surface temperatures reach high values quickly. The behavior of the surface temperature agrees with that reported by the first model. It is noticeable that the difference between the surface-averaged and the mass-averaged temperatures decreases along the axial distance, even though the values of both temperatures have been increased. In the case of high injection temperature and low ambient temperature, the surface- and mass-averaged

temperatures have a lower value than the injection temperature since energy has been transferred to the carrier gas.

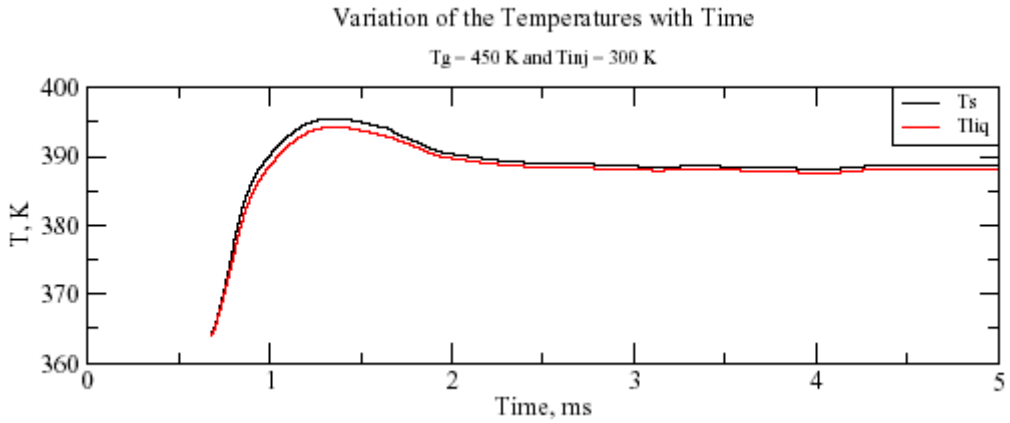

Figure 4. Variation of the Surface-Averaged and Mass-Averaged Temperatures with Time. (Model 2)

Sauter Mean Radius and Fuel Vapor Mass Fraction

The first case considered in this model has a spray injected at a relatively low temperature, 293K, and a gaseous medium in which the temperature is varied from 293 to 650K. The SMR increases as the gas temperature is increased, which agrees well with that obtained by the first model. The SMR, Figure 5a, is seen to be much higher for the cases in which the injection temperature is lower than the saturation temperature. The SMR for this model shows a slight decrease compared with that of the first model, but this is due to the lower value of the temperature difference between the surface temperature and the gas temperature. The FVMF, Figure 6a, shows an exponential increase as is reported for the first model.

When the liquid is injected at the saturation temperature the SMR, Figure 5b, is much lower than the first case since the large droplets evaporate more quickly. These results agree with those obtained in the first model. The behavior of the fuel vapor mass fraction, Figure 6b, also agrees with that reported in the first model but the values reported are slightly lower. This is due to the surface temperature having a lower value and, therefore, the temperature difference between the gas and the liquid is greater, which reflects in a longer time to heat up the droplet and also to evaporate it. However, by comparing this FVMF with that from the case of a lower injection temperature an increase is clearly seen since evaporation conditions are immediately reached after the injection.

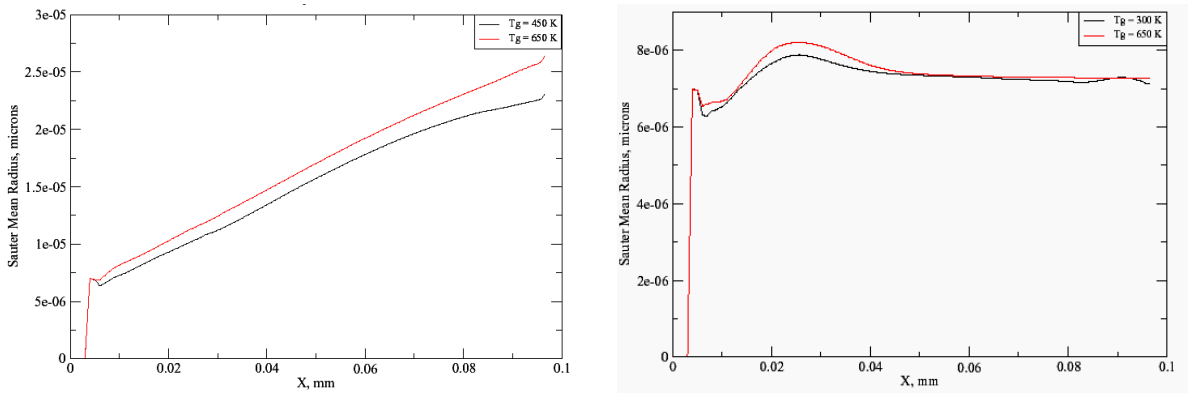

Figure 5. Variation of the SMR along the Axial Distance: a) T_{inj} = 300K and b) T_{inj} = 650K.

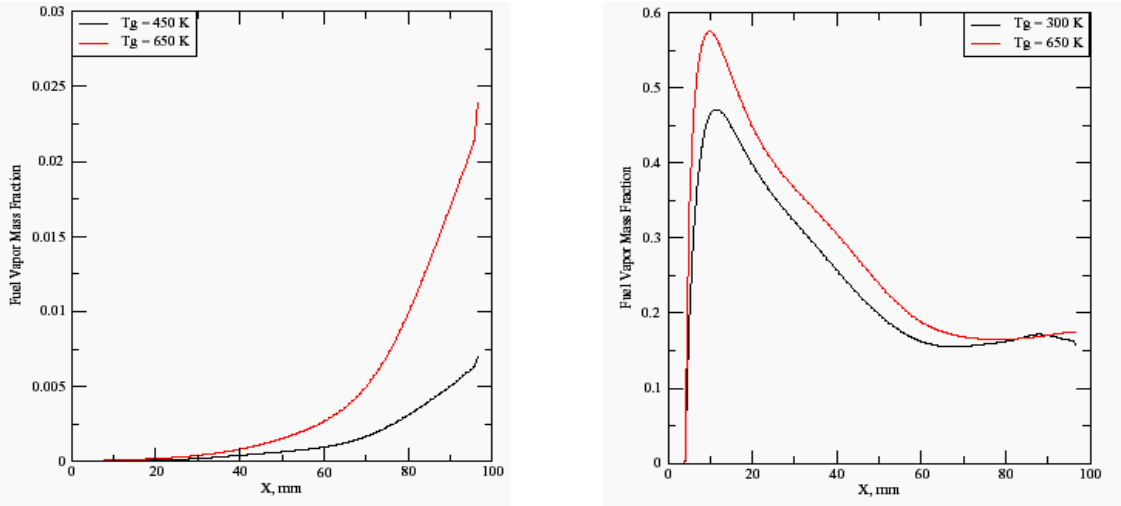

Figure 6. Variation of the FVMF along the Axial Distance: a) T_{inj} = 300K and b) T_{inj} = 650K.

6. Conclusions

Two methods of evaluating the surface-averaged temperatures in a spray, in the context of a spray model based on the evaluation of drop size moments, have been presented. The initial verifications shown here indicate that both methods work well, and give results that agree both between themselves and qualitatively with other models. Further work is required before firm conclusions can be drawn on the relative merits of the methods. This should including comparisons with experimental data and analyses of sprays with larger SMRs in which the differences between the surface-averaged and mass-averaged temperatures could be expected to be much larger.

Nomenclature

B_M	Mass Transfer Number
c_p	Specific Heat Capacity
D	Diameter
D_c	Diffusivity
h	Convective Heat Transfer Coefficient
k	Thermal Conductivity
L	Latent Heat of Vaporization
$\dot{m}$	Fuel Vapor Mass
$n(r)$	Number Size Distribution
Pr	Prandtl Number
r	Droplet Radius
Re	Reynolds Number
T	Temperature
U	Velocity
x	Coordinate Direction

Greek Symbols

ν	Kinematic Viscosity
ρ	Density

Subscripts/Superscripts

ev	Evaporative
g	Gas, Mixture
inj	Injection
j	Vector (Free) Index
k	Group of Droplets
l	Liquid
s	Droplet Surface

References

[1] Beck J C and Watkins A P 2003 Proc. R. Soc. Lond. A **459** 1 – 30.
[2] Beck J C and Watkins A P 2003 Int. J. of Heat Fluid Flow **24** 242 – 259.
[3] Ranz W E and Marshall W P 1952 Chem. Eng. Progress, Part I, **48** 141 – 146.
[4] Chin J S and Lefebvre A H 1985 Int. J. Turbo Jet Engines **2** 315 – 325.
[5] Melville W K and Bray K N C 1979 Int. J. Heat and Mass Transfer **22** 647 – 656.
[6] Beck J C and Watkins A P 2003 J. Comput. Phys. **182** 586 – 621.
[7] Abramzon B and Sirignano W A 1989 Int. J. Heat and Mass Transfer **32** 1605 – 1618.
[8] Daïf A, Bouaziz M, Chesneau X and Ali Chérif A 1999 Experimental Thermal and Fluid Science **18** 282 – 290.